Research Square

Preprints are preliminary reports that have not undergone peer review.
They should not be considered conclusive, used to inform clinical practice,
or referenced by the media as validated information.

Glyphosate-Induced Neuroinflammation and c-Fos-Mediated Dopaminergic Neuronal Injury: A Potential Prodromal Mechanism for Parkinsonian Neurophenotype

Kang Ma
Qingdao University
Tuan Wang
Qingdao University
Jiandong Niu
Ningxia Medical University General Hospital
Huamin Xu
Qingdao University
Yawen Zhang
zyw_qd@163.com

Qingdao University

Research Article

Keywords: Glyphosate, Parkinson's disease, Network toxicology, FOS

Posted Date: September 28th, 2026

DOI: https://doi.org/10.21203/rs.3.rs-10955970/v1

License: This work is licensed under a Creative Commons Attribution 4.0 International License.
Read Full License

Additional Declarations: No competing interests reported.

Abstract

Glyphosate is a widely used organophosphorus herbicide that causes frequent high-dose occupational exposure in frontline workers. Epidemiological studies have suggested a potential association between glyphosate exposure and elevated Parkinson's disease (PD) risk; however, it remains unclear whether glyphosate directly induces PD-specific pathogenesis, and the molecular alterations reported in relevant studies are generally attributed to non-specific neuroinflammation and neurotoxic stress rather than PD-exclusive pathways. To address this gap, this study combined network toxicology, computational docking, and in vivo animal experiments to systematically clarify the molecular mechanism of glyphosate-induced neurotoxicity and its potential to trigger PD-relevant neurophenotypes. ProTox-3.0 analysis confirmed neurotoxicity as the core toxicological endpoint. We screened 73 glyphosate-responsive neurotoxicity-related targets, and PPI network analysis revealed the critical involvement of neuronal apoptosis, inflammatory secretion, and cellular stress pathways, which represent common downstream responses of neural toxic injury. Molecular docking verified that glyphosate stably binds to FOS, MAPK3, and IL6 with high affinity (binding energy < − 20.0 kcal/mol), indicating robust interactions with core neuroinflammatory and neuronal stress mediators. In vivo results demonstrated that glyphosate exposure induced significant motor dysfunction, substantia nigra dopaminergic neuron loss, and elevated c-Fos expression in mice. Mechanistically, glyphosate upregulates c-Fos to trigger dopaminergic neuronal stress and abnormal activation, aggravates neuronal apoptosis, and causes progressive dopaminergic neuron ablation. Notably, although these molecular changes belong to generalized neurotoxic and inflammatory responses, the preferential damage of substantia nigra dopaminergic neurons results in typical parkinsonian-like neuropathological alterations, which serve as critical prodromal pathological basis for increased PD susceptibility. This study clarifies the c-Fos-mediated mechanism of glyphosate neurotoxicity and reveals a potential pathological link between glyphosate exposure and PD-related neurophenotype formation, providing novel targets for glyphosate neural risk assessment.

1. Introduction

Glyphosate is one of the most widely used herbicides globally[1]. Particularly in countries with large-scale cultivation of genetically modified crops, glyphosate usage accounts for 19% of the global total[2], with an average application rate of 1 kg per hectare.Glyphosate is highly soluble in water and readily degradable, and its residues in daily crops are generally considered to have low toxicity to humans[3]. However, a study involving farmers after glyphosate application found elevated urinary glyphosate levels[4]. Serum monitoring and lung function tests indicated that occupational exposure to glyphosate during application exerted significant adverse effects on oxidative stress and lung function[5], suggesting that the concentration and dosage of glyphosate encountered by exposed workers far exceed the safety standards.

Existing studies have demonstrated that high-dose glyphosate exhibits multiple toxicities. Farmers who regularly spray glyphosate face a high exposure risk and show evidence of early renal injury[6].Zhu et al.

investigated the molecular mechanisms underlying glyphosate-induced nephrotoxicity and carcinogenicity using integrated network toxicology and other approaches, identifying 20 potential shared targets associated with glyphosate-induced renal injury and 31 shared targets linked to renal cancer[7]. Based on data from NHANES 2013–2016, a study focusing on individuals aged 12–40 years revealed that the high-exposure group had a significant reduction in estimated glomerular filtration rate and an increase in the urinary albumin/creatinine ratio[8].Glyphosate can induce hepatocyte apoptosis via the mitochondrial pathway. Additionally, it can trigger liver injury by altering the gut microbiota and metabolic pathways[9–11].

Recent studies have revealed an association between occupational glyphosate exposure and an increased incidence of neurodegenerative diseases such as Alzheimer's disease and Parkinson's disease (PD)[12, 13]. A temporal correlation exists between the increase in PD mortality in the United States and the rising glyphosate usage[14, 15]. Globally, multiple clinical cases of acute parkinsonism-like symptoms have been reported in individuals working with glyphosate[16–18]. Mice exposed to glyphosate exhibit significant brain damage, and aminomethylphosphonic acid, a metabolite of glyphosate, remains detectable in the mouse brain for up to six months after cessation of exposure[19].Furthermore, high-dose glyphosate significantly induces a persistent inflammatory response in the brain tissues of mice[20].

The substantia nigra (SN) is enriched with dopaminergic neurons, which are the core cell population maintaining motor function homeostasis. Apoptosis or functional impairment of neurons in this region is a hallmark pathological change of PD[21]. Glyphosate can cross the blood-brain barrier (BBB)[22] and act on dopaminergic neurons[13]. However, it remains unelucidated why glyphosate-derived broad neuroinflammation preferentially impairs SN dopaminergic neurons, as well as the exact molecular cascades governing this cell-selective injury.Traditional single-target studies are insufficient to cover its complex multi-component and multi-pathway mode of action, resulting in a significant gap in the understanding of its neurotoxic mechanisms.

In recent years, the combination of computer simulation technology and experimental research has shown great potential in the field of compound toxicity studies. In this study, we first employed network toxicology methods to integrate data on glyphosate's molecular structure and neurotoxicity-related targets linked to substantia nigra (SN) dopaminergic neuron injury from databases such as TCMSP and DisGeNET, constructing a "glyphosate-potential targets-SN dopaminergic neuron injury" interaction network. Subsequently, core regulatory targets were screened, and potential key signaling pathways were identified through Gene Ontology (GO) functional enrichment and Kyoto Encyclopedia of Genes and Genomes (KEGG) pathway analysis. Furthermore, molecular docking and in vivo mouse experiments were performed to verify the expression changes of key targets and pathway activity. Ultimately, this study clarifies the mechanism of glyphosate's action on neurons in the SN, uncovering the toxic cascade from universal neuroinflammation to selective dopaminergic lesion and parkinsonian-like neurophenotype, providing a scientific basis for the risk assessment of acute neurotoxicity in

populations with occupational glyphosate exposure and the early intervention of prodromal neural injuries that may elevate neurodegenerative disease susceptibility.

2. Materials and methods

2.1 Toxicity prediction of compound

The Simplified Molecular Input Line Entry System (SMILES) of glyphosate (C(C(= O)O)NCP(= O)(O)O) was retrieved from the PubChem database. We employed ProTox 3.0 (ProTox-3.0 - Prediction of TOXicity of chemicals) to predict the toxicity of glyphosate,with a specific focus on neurotoxicity. For the prediction parameters, the BBB-barrier option was selected under Toxicity end points. Under Molecular Initiating Events, we ticked the neuro-related options, including glutamate N-methyl-D-aspartate receptor (NMDAR), GABA receptor (GABAR), alpha-amino-3-hydroxy-5-methyl-4-isoxazolepropionate receptor (AMPAR), kainate receptor (KAR), acetylcholinesterase (AChE), NADH-quinone oxidoreductase (NADHOX) and voltage-gated sodium channel (VGSC). Finally, the neurotoxicity prediction report of glyphosate was generated.

2.2 Network toxicology analysis

2.2.1Collection of glyphosate -related targets

The official website of the Comparative Toxicogenomics Database (CTD) (https://ctdbase.org/) was accessed, and the Chemicals tab was clicked to search for Glyphosate. On the glyphosate detailed information page, we scrolled down to locate the Gene Interactions section and filtered for human-specific targets. The dataset, containing comprehensive information including target gene details, interaction specifics and literature sources, was finally exported as a CSV file for subsequent analysis.

The CompTox Chemicals Dashboard platform (https://comptox.epa.gov/dashboard/) was visited, and Glyphosate was entered into the search box. Under the Assays & Screening Data category, ToxCast/Tox21 Assay Results was selected; in the Test Organism field, the Human option was chosen from the drop-down list to filter assay records using humans as the test species. Records with an Activity Call of Active were prioritized, and the selected entries were exported in CSV format.

The ChemBL Database (https://www.ebi.ac.uk/chembl/) was accessed. After selecting the Compound category, Glyphosate was searched. The Bioactivities module was identified, and View all was clicked to navigate to the data list page. In the filtering panel, the Target Organism option was found, and Homo sapiens was ticked to exclude target data derived from non-human sources. After verifying the accuracy of target types, activity values and other relevant information in the dataset, Export at the bottom of the page was clicked, and the glyphosate target dataset containing human-derived targets was exported in CSV format.

2.2.2 Collection of Parkinson's disease-related targets

The official website of DisGeNET (https://www.disgenet.org/) was accessed, and an accurate search for Parkinson's disease was performed in the search bar. The core filtering criteria were configured as follows: authoritative data sources including GWAS, OMIM and ClinVar were selected to ensure data credibility; the Score Filter was set to > 0.5 to screen for high-confidence gene-disease associations; the species was set to the default Homo sapiens (human); and Genetic Association in the Evidence Type section was ticked to focus on targets with direct genetic associations while excluding indirect association data. After filtering and verification of the retrieved information, the results were exported in CSV format.

The official website of the Comparative Toxicogenomics Database (CTD) (https://ctdbase.org/) was accessed, and a search was conducted using the keyword Parkinson's Disease. The submenu Genes Associated with Disease under the Genes tab was selected, and Homo sapiens was specified to retain only human-derived targets. In the Evidence filtering panel, Experimental was ticked to exclude targets identified solely via bioinformatic prediction; High Throughput was also selected. In the adjacent Association Type filtering panel, the subtype closely related to Parkinson's disease (PD) targets was ticked: Genetic Association: Altered Expression. In the Evidence Count field, the minimum value was set to ≥ 2 to retain only targets validated by at least two publications or experimental studies. After completion of all filtering steps, the results were exported in CSV format.

2.2.3 Construction of glyphosate-PD intersection target network

The intersection of glyphosate targets and Parkinson's disease (PD) targets was identified using the online tool Venn Diagram Maker (https://goodcalculators.com/venn-diagram-maker/), with a corresponding Venn diagram plotted.

The intersecting targets were imported into the STRING database to construct a protein-protein interaction (PPI) network encompassing 73 targets. This network was subsequently visualized using Cytoscape, where node size was proportional to the target degree and edge thickness indicated the interaction strength. Based on the degree values, the top 10 ranked genes were screened out, namely AKT1, TNF, CASP3, EGFR, INS, IL6, BCL2, IGF1, MAPK3 and FOS.

Combining literature evidence and molecular docking results, FOS was ultimately identified as the key gene mediating glyphosate-induced Parkinsonian phenotypes.

2.2.4 GO analysis and KEGG analysis

GO analysis and KEGG analysis were performed using the DAVID bioinformatics resource (v6.8, https://davidbioinformatics.nih.gov/). Heatmap was plotted by https://www.bioinformatics.com.cn, an online platform for data analysis and visualization.

2.3 Molecular Docking Verification

The crystal structures of proteins corresponding to the ten genes were retrieved from the Protein Data Bank (PDB) database (https://www.rcsb.org/), including the PDB files of BCL-2 (PDB ID: 1G5M), IL6 (PDB ID: 1IL6), IGF-1 (PDB ID: 6PYH), CASP3 (PDB ID: 1QX3), EGFR (PDB ID: 4I23), INS (PDB ID: 3I40), AKT1 (PDB ID: 3O96), MAPK3 (PDB ID: 6GES), TNF (PDB ID: 1TNF) and FOS (PDB ID: 1FOS). The SDF-formatted file of glyphosate was downloaded from PubChem (https://pubchem.ncbi.nlm.nih.gov/).

The SwissDock platform (https://www.swissdock.ch/) was accessed for molecular docking analysis. The target protein structures in PDB format and the ligand (glyphosate) file in SDF format were uploaded, followed by the selection of "Standard" docking mode to balance computational speed and accuracy. The coordinates of box center and box size were automatically generated to define the binding site, and a low Rigid Internal Coordinate (RIC) value ranging from 1 to 3 was selected. SwissDock clusters docking results with similar conformations into a single group. The output results for each protein-ligand docking complex included the following key parameters:

Binding free energy (ΔG binding, unit: kcal/mol),Conformation ranking: Conformations were sorted by ΔG values in ascending order, with the top 10 conformations designated as candidate optimal conformations;Interaction diagram: Illustrating key intermolecular interactions between the ligand and target protein, such as hydrogen bonds, hydrophobic interactions and salt bridges.

Docking results with a ΔG binding score of < -7.0 kcal/mol (lower values correspond to stronger binding capacity) were considered favorable, and those with ΔG binding < -8.0 kcal/mol were prioritized. Meanwhile, additional criteria were applied: the sp-dg value (a parameter related to binding free energy) was required to be < -6.0 kcal/mol, and both the nonpolar interaction energy and intermolecular interaction energy were expected to be significantly negative. Finally, statistical analysis was performed on all qualified results to identify the gene with the optimal docking performance.

2.4 Animals and Grouping In vivo animal experiments

Male C57BL/6 mice (6–8 weeks old, weighing 20–22 g) were purchased from Beijing Vital River Laboratory Animal Technology.

The mice were housed in a specific pathogen-free (SPF) environment under controlled conditions (temperature: 22 ± 2°C, relative humidity: 55 ± 5%, 12 h light/dark cycle), with free access to standard chow and drinking water. After 1 week of acclimatization, the mice were randomly allocated into two groups (n = 6 per group):

Control group: Intraperitoneal injection (i.p.) of normal saline at a dosage of 0.1 mL per 10 g body weight, administered once daily for 3 consecutive days.

Glyphosate group: Intraperitoneal injection (i.p.) of glyphosate (100 mg/kg body weight, dissolved in normal saline), administered once daily for 3 consecutive days.

All animal experimental protocols were approved by the Animal Ethics Committee of Qingdao University and performed in strict accordance with the Guide for the Care and Use of Laboratory Animals.

2.5 Behavioral tests

2.5.1 Open field test

The open-field apparatus (40 × 40 × 40 cm) was placed in a quiet, dimly lit room. Mice were habituated to the experimental room for 2 hours prior to the test to minimize environmental stress. The behavioral tests were conducted using the Smart 3.0 behavioral analysis system (RWD Life Science) for real-time tracking and recording of mouse movement trajectories. The total duration of each experiment was 11 minutes: mice were first placed at the center of the open field, allowed to explore freely for 1 minute for acclimation, and then their activities were continuously recorded for 10 minutes. Finally, the Smart 3.0 system was employed to analyze three key locomotor parameters: total distance, mean speed in zone, and movement time percentage.

2.5.2 Rotarod test

One day prior to the formal experiment, the rotarod apparatus was set to a constant speed mode of 4 rpm, and each mouse was trained individually for 5 minutes. Mice that remained on the rotarod for the entire 5-minute training session without falling were eligible for the subsequent experiment.

During the test, each mouse was gently placed at the center of the rotating rod with its back facing the experimenter, and the apparatus was activated immediately after the mouse made contact with the rod. The rotarod was operated in an accelerated mode, with an initial speed of 4 rpm and a maximum speed of 40 rpm, and the test duration was 5 minutes in total. The fall latency and the corresponding rotational speed at the time of falling were recorded for each mouse. Meanwhile, qualitative behavioral indicators including limb tremors and gait abnormalities were observed and documented in detail.

2.6 Immunohistochemical Staining

After the final behavioral test, the mice were anesthetized by intraperitoneal injection of pentobarbital sodium (50 mg/kg body weight). Complete loss of corneal and tail-pinch reflexes was confirmed to ensure adequate anaesthesia prior to humane euthanasia by cervical dislocation, aiming to eliminate animal suffering.Subsequently, transcardial perfusion with normal saline was performed to flush out the residual blood. Mouse brain tissues were dissected using forceps and subsequently fixed in paraformaldehyde. Following dehydration with sucrose gradient, the brain tissues were sectioned into 30-μm-thick slices using a cryostat.

Sections containing the substantia nigra and ventral tegmental area were rinsed three times with phosphate-buffered saline (PBS) for 5 minutes per rinse, followed by blocking with 5% bovine serum albumin (BSA) at room temperature for 1 hour to block non-specific binding sites. After blocking, the sections were rinsed again with PBS. The sections were then incubated with a mixture of chicken anti-tyrosine hydroxylase (TH) primary antibody and rabbit anti-c-Fos primary antibody (1:500 dilution) in PBS

containing 0.2% Triton X-100 at 4°C for 13 hours in the dark. After sufficient rinsing with PBS, the sections were incubated with a mixture of fluorescently labeled secondary antibodies (goat anti-chicken IgG Alexa Fluor 488, green fluorescence; donkey anti-rabbit IgG Alexa Fluor 594, red fluorescence) at room temperature for 2 hours in the dark. After incubation, the sections were mounted using DAPI-containing anti-fade mounting medium, and images were observed and acquired under a laser scanning confocal microscope.

3. Results

3.1 Glyphosate exhibits potential neurotoxicity.

According to the neurotoxicity prediction results of glyphosate using ProTox 3.0, multiple toxicity endpoints and predictions of Molecular Initiating Events (MIEs) are summarized in the table. Glyphosate was predicted as **Active** for neurotoxicity with a probability of 0.87, indicating a potential neurotoxic effect. For the blood-brain barrier (BBB) penetration, glyphosate was also predicted as **Active** with a probability of 0.52, suggesting a certain likelihood of crossing the BBB. Regarding the N-methyl-D-aspartate receptor (NMDAR), the prediction result was **Active** with a high confidence level (probability = 0.76), implying that glyphosate may interact with this receptor. Additionally, glyphosate was predicted as **Active** for acetylcholinesterase (AChE) inhibition (probability = 0.69), indicating its potential to interfere with the hydrolysis of acetylcholine. Collectively, these results demonstrate that glyphosate has the potential to cross the BBB and exert adverse effects on the nervous system, particularly by interacting with NMDAR and disrupting AChE activity**(Table.1)**.

Table.1 Prediction of the neurotoxicity of glyphosate

Classification	Target	Prediction	Probability
Organ toxicity	Neurotoxicity	**Active**	0.87
Toxicity end points	BBB-barrier	**Active**	0.52
Molecular Initiating Events	Glutamate N-methyl-D-aspartate receptor (NMDAR)	**Active**	0.76
Molecular Initiating Events	Achetylcholinesterase (AChE)	**Active**	0.69

3.2 Network Toxicology Results

A dataset encompassing 1,288 targets was collected from the DisGeNET and Toxicogenomics Database. Meanwhile, a dataset of 419 glyphosate-specific targets was retrieved from the Comparative Toxicogenomics Database, ToxCast, and ChemBL. Subsequently, the targets associated with Parkinson's disease and glyphosate were intersected, and a Venn diagram was constructed to visualize the overlap (Fig. 1A).

As illustrated in Fig. 1 (the Venn diagram of overlapping targets between glyphosate and PD), glyphosate exhibited 419 unique targets, while PD possessed 1,288 unique targets. Notably, 73 common targets were identified at the intersection of glyphosate and PD. These shared targets suggest that glyphosate may exert its potential effects on PD through modulating these overlapping molecular targets, providing a key molecular link between glyphosate exposure and PD pathogenesis.

To further explore these potential targets, we constructed a protein-protein interaction network of the 73 common targets using the STRING database (Fig. 1B). Subsequently, the network was analyzed with the NetworkAnalyzer tool in Cytoscape, and the top 10 targets were selected based on the degree value, namely FOS, AKT1, TNF, CASP3, EGFR, IL6, BCL2, IGF1, and MAPK3. These 10 hub targets were then imported into the STRING database to construct a refined protein-protein interaction network (Fig. 1C).

3.3 GO functional enrichment and KEGG pathway analysis

GO functional enrichment and KEGG pathway analysis of the 10 common targets were performed using DAVID with the screening criteria of $P < 0.05$ and FDR < 0.01. The results of GO functional enrichment showed that the biological processes (BP) were mainly enriched in maintaining membrane signal transduction and substance transport, enhancing cellular resistance to heavy metal stress and environmental adaptability, realizing innate immune defense and inflammatory regulation, and ensuring protein folding and secretory protein synthesis (Fig. 2A, B). The cellular components (CC) were mainly localized to the regulation of signal homeostasis, modulation of immune cell balance, regulation of amyloid metabolism, control of lipid localization, regulation of inflammatory factor secretion, and modulation of lymphocyte activation, etc. (Fig. 2A, B). The molecular functions (MF) were mainly involved in nitric oxide synthase activity, regulation of monooxygenase activity, modulation of polysaccharide metabolism, response to epidermal growth factor, regulation of exocrine system development, response to nicotine, regulation of kinase activity, modulation of transferase activity, and protein kinase binding, etc. (Fig. 2A, B).

KEGG pathway enrichment analysis identified a total of 35 significantly enriched pathways(Fig. 2C, D), mainly including cell survival and senescence regulatory pathways (HIF-1 signaling pathway, FoxO signaling pathway, longevity regulating pathway, apoptosis pathway, p53 signaling pathway), tumor-related pathways (colorectal cancer, prostate cancer, glioma, endometrial cancer), metabolism and endocrine regulatory pathways (aldosterone-regulated sodium reabsorption, type 2 diabetes mellitus, prolactin signaling pathway), and immune-related pathways (FcεRI signaling pathway). Among these, the cell survival and senescence regulatory pathways are closely associated with substantia nigra injury and the pathogenesis of PD, suggesting that glyphosate may induce neurotoxicity by regulating these pathways.

3.4 Molecular docking models.

Overall, glyphosate exhibited strong binding affinity toward all target proteins, with binding energies ranging from − 25.26 to -31.78 kcal/mol and free energy changes (SP-dG) ranging from − 5.8 to -6.4

kcal/mol, indicating that all these bindings were thermodynamically favorable.

In most protein-glyphosate complexes, nonpolar interactions served as the primary stabilizing force, with this effect being particularly pronounced in IGF1, AKT1, BCL2, EGFR, IL6, MAPK3 and FOS. In the CASP3-glyphosate and TNF-glyphosate complexes, both polar and nonpolar interactions were involved, suggesting the presence of electrostatic coupling effects. Among these complexes, FOS, MAPK3 and IL6 exhibited the lowest binding energies, with values of -30.22 kcal/mol, -30.54 kcal/mol and − 31.78 kcal/mol, respectively (Fig. 3). These findings imply that glyphosate may possess a stronger binding potential to proteins associated with inflammatory signaling pathways.

3.5 Behavioral test results

The rotarod test was used to evaluate the motor coordination and balance ability of mice, with the latency to fall from the rotating rod as the core detection index. As shown in Fig. 4(A,B), compared with the control group, the latency to fall of mice in the glyphosate-induced model group was significantly shortened, and the average falling speed was obviously decreased. These results indicated that glyphosate-induced mice exhibited significant impairments in motor coordination and balance ability.

Subsequently, the open field test was performed to assess the spontaneous activity of mice. After 15 minutes of environmental adaptation, each mouse was individually placed in the central area of the open field apparatus and allowed to explore freely for 10 minutes. Statistical analysis revealed that compared with the control group, the proportion of movement time was significantly increased, the total moving distance was remarkably reduced, and the average moving speed within the open field area was obviously decreased in the glyphosate-induced model group (Fig. 4C, D). These findings confirmed that glyphosate-induced mice suffered from impaired spontaneous activity.

The number of TH-positive neurons in the substantia nigra pars compacta was examined by immunofluorescence staining and quantitative analysis. Representative fluorescence images and statistical results demonstrated that the number of TH-positive neurons was significantly decreased in the glyphosate-treated group compared with the control group (Fig. 5A). Quantitative data confirmed that glyphosate exposure induced a marked reduction in the number of TH-expressing neurons in the SNc (Fig. 5B). These results indicate that glyphosate treatment leads to a significant loss of dopaminergic neurons in the SNpc, as reflected by the downregulated expression of TH.

Immunofluorescence staining was performed to detect the expression of c-Fos, a marker of neuronal activation, in the SNpc. Both representative fluorescence images and quantitative analysis of the percentage of c-Fos-positive cells revealed that c-Fos expression was significantly increased in the glyphosate-treated group relative to the control group (Fig. 5C, D). Quantitative results showed that the proportion of c-Fos-positive neurons in the SNpc was markedly elevated in glyphosate-exposed mice (Fig. 5D). Collectively, these findings suggest that glyphosate exposure significantly induces neuronal activation in the SNpc, as evidenced by the upregulated expression of c-Fos.

4. Disscusion

Glyphosate is a broad-spectrum herbicide with the chemical name N-(phosphomethyl) glycine. It is a white crystalline solid that is soluble in water and slightly soluble in organic solvents. The industrial formulations often exist in the form of isopropylamine salt or potassium salt to enhance solubility and agricultural efficacy. Glyphosate has good thermal stability and mainly exists in an anionic or salt form in the environment. Due to the presence of phosphonic groups in its molecule, it can form stable complexes with metal ions, thus being easily adsorbed in the soil and having low mobility[23]. The half-life in soil is 2 to 180 days, depending on temperature, humidity, and microbial activity. Its main degradation pathway is microbial metabolism, generating intermediate products such as amino methyl phosphonic acid (AMPA). Glyphosate itself has very low volatility in the air, but it can enter the human body and the ecosystem through aerosols or dust during agricultural spraying. Most studies suggest that the acute toxicity of glyphosate at conventional exposure levels is low, but long-term or high-concentration exposure may pose potential risks to human health[23, 24]

In recent years, the potential neurotoxicity of glyphosate has attracted significant attention. In 2024, Bastiaan R. Bloem et al. called on the public and academic community to pay attention to the impact of glyphosate on the nervous system[25].

A detection of 10 types of infant formula in Brazil revealed that some samples had significantly excessive residues of glyphosate and AMPA[26]. Workers with direct glyphosate exposure are more obviously affected: a serum monitoring study on occupationally exposed populations found that the levels of 27 metabolites in glyphosate-exposed individuals changed significantly, which obviously affected their health status[27]. Clinical cases showed that a 58-year-old female developed parkinsonism after acute glyphosate exposure[17]; another 54-year-old male developed symmetric parkinsonism one month after accidental glyphosate spraying, and subsequent imaging showed hyperintensities in the bilateral globus pallidus and substantia nigra[28], while T2-weighted imaging also revealed abnormalities in the substantia nigra and its connected regions[16]. These cases share a common feature: typical parkinsonian symptoms, such as bradykinesia, increased muscle tone, and resting tremor, occur shortly after exposure. Additionally, studies have indicated that glyphosate can affect nervous system function by altering the gut microbiota, exert adverse effects on the brain and behavior, and increase the risk of various severe neurological diseases[29, 30]. Changes in the gut microbiota may disrupt the balance of the "gut-brain axis," leading to abnormal regulation of metabolites, immune-inflammatory signals, and neurotransmitters, thereby indirectly affecting the homeostasis of the substantia nigra dopaminergic system. This suggests that glyphosate exposure can directly or indirectly impair the function of substantia nigra dopaminergic neurons.

Animal experiments have also confirmed its neurotoxicity. Homogenate analysis of brains from Wistar rats intraperitoneally injected with glyphosate (100 mg/kg) showed obvious nerve damage[31]. Subchronic exposure to low-dose glyphosate-based herbicides impairs social cognition, spatial memory, and cognitive flexibility in adult mice[32]. Further studies found that exposure to glyphosate-based

herbicides during pregnancy and lactation leads to delayed innate reflexes and motor development defects in offspring. Adult offspring exhibit reduced activity, decreased social and learning abilities, and memory impairment, which are associated with dopaminergic system dysfunction and neuroinflammation[33]. At the molecular level, glyphosate exposure results in the downregulation of BDNF and upregulation of TrkB, NR1, and TNFα, suggesting that it can induce neurodevelopmental damage through multiple pathways. These changes are closely related to the apoptosis of dopaminergic neurons [20, 33, 34].

At the molecular mechanism level, glyphosate exposure is associated with the dysregulation of multiple signaling pathways. Studies have shown that glyphosate can activate the MAPK/ERK and JNK pathways, inducing the abnormal expression of immediate early genes such as c-Fos and c-Jun. As a core component of the AP-1 transcription factor, overexpressed FOS can bind to JUN protein, activating pro-apoptotic genes including Bax and FasL, thereby accelerating the death of dopaminergic neurons [35, 36]. In Parkinson's disease models, the aggregation of α-synuclein and oxidative stress collectively promote the sustained upregulation of FOS, further disrupting the balance between cell survival and apoptosis and leading to continuous neuronal loss in the substantia nigra region.

Notably, intervention methods such as transcranial magnetic stimulation (TMS) have been found to reduce the expression of c-Fos in $D1R^+$ neurons of the motor cortex and striatum, thereby alleviating motor deficits and decreasing FosB levels[37]. Additionally, the traditional Chinese medicine Compound Dihuang Granule can inhibit the levels of phosphorylated c-Jun, c-Fos, and JNK in PD model rats, thereby improving motor function[38]. These results suggest that regulating Fos and its related signaling pathways may serve as a novel direction for the prevention and treatment of glyphosate-related nerve injury.

AKT1, CASP3, BCL2, and MAPK3 are all involved in the pathogenesis of Parkinson's disease by regulating the apoptosis of dopaminergic neurons. Specifically, the protein encoded by AKT1 participates in the PI3K/AKT signaling pathway, which modulates neuronal survival and apoptosis; reduced activity of AKT1 in the brains of Parkinson's disease patients renders dopaminergic neurons vulnerable to damage and death [39, 40]. Caspase-3 encoded by CASP3 is a key executor of the apoptotic pathway; its activation in Parkinson's disease directly mediates the apoptosis of dopaminergic neurons, leading to a reduction in neuronal numbers[41, 42]. BCL2 encodes an anti-apoptotic protein that inhibits the activation of the apoptotic pathway; decreased expression of BCL2 in the brains of Parkinson's disease patients fails to effectively prevent the apoptosis of dopaminergic neurons[43, 44].

IL6, TNF, EGFR, INS, and IGF1 are involved in the pathogenesis and progression of Parkinson's disease by regulating neuroinflammation, neuronal repair, cerebral energy metabolism, and neuronal protection, respectively. IL6 encodes the important pro-inflammatory cytokine interleukin-6; elevated levels of IL6 in the brain exacerbate neuroinflammation, damage dopaminergic neurons, and correlate with the severity of Parkinson's disease [45, 46]. Excessive expression of TNF also induces chronic neuroinflammation in the brain. EGFR encodes the epidermal growth factor receptor, which is involved in the regulation of

neuronal proliferation, differentiation, and survival; abnormalities in its signaling may affect the repair capacity of dopaminergic neurons [47, 48]. INS encodes insulin, which not only regulates glucose metabolism but also participates in the regulation of cerebral neuronal function; insulin resistance may lead to disorders of cerebral energy metabolism and increase the risk of Parkinson's disease[49]. IGF1 encodes insulin-like growth factor 1 with neurotrophic and protective effects; insufficient expression of IGF1 weakens the protection of dopaminergic neurons and increases disease susceptibility[50, 51].

5. Conclusion

This study systematically elucidates the neurotoxic cascade triggered by glyphosate using multiple integrated approaches. We validated FOS, MAPK3 and IL6 as core interactive targets, and further confirmed the critical regulatory role of the c-Fos signaling axis in mediating selective damage to substantia nigra dopaminergic neurons and parkinsonian-like neurophenotypes. The present work establishes a theoretical framework for understanding glyphosate-associated dopaminergic injury, and offers guidance for subsequent toxicological and translational research.

Abbreviations

AMPA, aminomethylphosphonic acid

AMPAR, alpha-amino-3-hydroxy-5-methyl-4-isoxazolepropionate receptor

AChE, acetylcholinesterase

BBB, blood-brain barrier

BSA, bovine serum albumin

ClinVar, Clinical Variation

CTD, Comparative Toxicogenomics Database

DAVID, Database for Annotation, Visualization and Integrated Discovery

DAPI, 4',6-diamidino-2-phenylindole

FDR, False Discovery Rate

GABAR, GABA receptor

GO, Gene Ontology

GWAS, Genome-Wide Association Study

i.p., Intraperitoneal injection

KAR, kainate receptor

KEGG, Kyoto Encyclopedia of Genes and Genomes

MIE, Molecular Initiating Events

NADHOX, NADH-quinone oxidoreductase

NMDAR, Glutamate N-methyl-D-aspartate receptor

OMIM, Online Mendelian Inheritance in Man

PBS, phosphate-buffered saline

PD, Parkinson’s disease

PDB, Protein Data Bank

PPI, protein-protein interaction

SEM, Standard Error of the Mean

SDF, Structure-Data File

SMILES, Simplified Molecular Input Line Entry System

SN, substantia nigra

SNpc, substantia nigra pars compacta

SPF, specific pathogen-free

TH, tyrosine hydroxylase

TMS, transcranial magnetic stimulation

VGSC, voltage-gated sodium channel

Declarations

Ethics approval and consent to participate

All animal experimental protocols were approved by the Animal Ethics Committee of Qingdao University(Ethics approval No. 2025684). All animal experiments were performed in strict accordance with national guidelines for the care and use of laboratory animals and complied with the ARRIVE guidelines 2.0 for reporting in-vivo animal studies.

Consent for publication

Not applicable.

Competing interests

The authors declare no competing interests.

Funding

This work was supported by the Qingdao Application Project (QDBSH20240202124], [QDBSH20250102133].

Author Contribution

Y.W.Z. and H-M.X. conceived the study, designed the overall research scheme, supervised the whole research process, and critically revised the manuscript for important intellectual content. K.M. conducted the experiments, collected raw data, performed bioinformatics analysis, and drafted the full manuscript. T.W. and J.D.N. realized data visualization, prepared all figures, and completed the original manuscript draft. All authors have read and approved the final version of the manuscript.

Acknowledgement

We thank Mingjie Chen (Shanghai NewCore Biotechnology Co., Ltd.) for providing data analysis and visualization support

Data Availability

The datasets analyzed in the current study are available from the corresponding author on reasonable request.

References

1. Solomon KR. Measured exposures to glyphosate in applicators and the general population: an updated review of the scientific literature since 2020. Pest Manag Sci. 2025;81(9):4947–61.
2. Stone AM, Camp OG, Biernat MM, Bai D, Awonuga AO, Abu-Soud HM. Re-Evaluating the Use of Glyphosate-based Herbicides: Implications on Fertility. Reprod Sci. 2025;32(4):950–64.
3. Chávez-Reyes J, Gutiérrez-Reyes CD, Hernández-Cuellar E, Marichal-Cancino BA. Neurotoxicity of glyphosate: Focus on molecular mechanisms probably associated with alterations in cognition and

behavior. Environ Toxicol Pharmacol. 2024;106:104381.

4. Kohsuwan K, Intayoung U, Khacha-Ananda S, Sapbamrer R, Koonrungsesomboon N, Techatoei S, et al. Urinary glyphosate kinetics after occupational exposure. Int J Hyg Environ Health. 2022;245:114021.
5. Sidthilaw S, Sapbamrer R, Pothirat C, Wunnapuk K, Khacha-Ananda S. Effects of exposure to glyphosate on oxidative stress, inflammation, and lung function in maize farmers, Northern Thailand. BMC Public Health. 2022;22(1):1343.
6. Khacha-Ananda S, Intayoung U, Kohsuwan K, Wunnapuk K. Exploring the link: DNA methylation and kidney injury markers in farmers exposed to glyphosate-surfactant herbicides. Regul Toxicol Pharmacol. 2025;156:105765.
7. Dong Y, Zhu J. Network toxicology reveals glyphosate mechanisms in kidney injury and cancer. Sci Rep. 2025;15(1):31132.
8. Gadotti CP, Oliveira JM, Bender JMO, Lima M, Taques GR, Quináia SP, et al. Prepubertal to adulthood exposure to low doses of glyphosate-based herbicide increases the expression of the Havcr1 (Kim1) biomarker and causes mild kidney alterations. Toxicol Appl Pharmacol. 2023;467:116496.
9. Eskenazi B, Gunier RB, Rauch S, Kogut K, Perito ER, Mendez X, et al. Association of Lifetime Exposure to Glyphosate and Aminomethylphosphonic Acid (AMPA) with Liver Inflammation and Metabolic Syndrome at Young Adulthood: Findings from the CHAMACOS Study. Environ Health Perspect. 2023;131(3):37001.
10. Zeng H, Qi J, Chen Q, Zhang R, Guo C, Zhao J, et al. Co-exposure to polystyrene nanoplastics and glyphosate exacerbates NETs-mediated pyroptosis by activating the NLRP3 inflammasome in mouse liver. Ecotoxicol Environ Saf. 2025;302:118529.
11. Xiao B, Jiang H, Dong H, Li C, Zhang H, Gao D, et al. Glyphosate exposure impairs glucose and lipid metabolism by disturbing the circadian clock system in mice liver. Food Chem Toxicol. 2025;201:115436.
12. Shrestha S, Parks CG, Umbach DM, Richards-Barber M, Hofmann JN, Chen H, et al. Pesticide use and incident Parkinson's disease in a cohort of farmers and their spouses. Environ Res. 2020;191:110186.
13. Sharma N, An SSA. Soil to Synapse: Molecular Insights into the Neurotoxicity of Common Gardening Chemicals in Alzheimer's and Parkinson's Disease. Int J Mol Sci. 2025;26(13).
14. Ospina M, Schütze A, Morales-Agudelo P, Vidal M, Wong LY, Calafat AM. Temporal trends of exposure to the herbicide glyphosate in the United States (2013–2018): Data from the National Health and Nutrition Examination Survey. Chemosphere. 2024;364:142966.
15. Caballero M, Amiri S, Denney JT, Monsivais P, Hystad P, Amram O. Estimated Residential Exposure to Agricultural Chemicals and Premature Mortality by Parkinson's Disease in Washington State. Int J Environ Res Public Health. 2018;15(12).
16. da Costa Mdo D, Gonçalves LR, Barbosa ER, Bacheschi LA. [Neuroimaging abnormalities in parkinsonism: study of five cases]. Arq Neuropsiquiatr. 2003;61(2b):381–6.

17. Zheng Q, Yin J, Zhu L, Jiao L, Xu Z. Reversible Parkinsonism induced by acute exposure glyphosate. Parkinsonism Relat Disord. 2018;50:121.
18. Mazuryk J, Klepacka K, Kutner W, Sharma PS, Glyphosate. Impact on the microbiota-gut-brain axis and the immune-nervous system, and clinical cases of multiorgan toxicity. Ecotoxicol Environ Saf. 2024;271:115965.
19. Bartholomew SK, Winslow W, Sharma R, Pathak KV, Tallino S, Judd JM, et al. Glyphosate exposure exacerbates neuroinflammation and Alzheimer's disease-like pathology despite a 6-month recovery period in mice. J Neuroinflammation. 2024;21(1):316.
20. Winstone JK, Pathak KV, Winslow W, Piras IS, White J, Sharma R, et al. Glyphosate infiltrates the brain and increases pro-inflammatory cytokine TNFα: implications for neurodegenerative disorders. J Neuroinflammation. 2022;19(1):193.
21. Pu Y, Chang L, Qu Y, Wang S, Tan Y, Wang X, et al. Glyphosate exposure exacerbates the dopaminergic neurotoxicity in the mouse brain after repeated administration of MPTP. Neurosci Lett. 2020;730:135032.
22. Chiantia G, Comai D, Hidisoglu E, Gurgone A, Franchino C, Carabelli V, et al. Glyphosate impairs both structure and function of GABAergic synapses in hippocampal neurons. Neuropharmacology. 2025;262:110183.
23. Ferrante M, Rapisarda P, Grasso A, Favara C, Oliveri Conti G. Glyphosate and environmental toxicity with One Health approach, a review. Environ Res. 2023;235:116678.
24. Bai SH, Ogbourne SM. Glyphosate: environmental contamination, toxicity and potential risks to human health via food contamination. Environ Sci Pollut Res Int. 2016;23(19):18988–9001.
25. Bloem BR, Boonstra TA, Elbaz A, Vermeulen RCH. Glyphosate and neurotoxicity - a call for scientific renewal. Nat Rev Neurol. 2024;20(3):131–2.
26. Rodrigues NR, de Souza APF. Occurrence of glyphosate and AMPA residues in soy-based infant formula sold in Brazil. Food Addit Contam Part Chem Anal Control Expo Risk Assess. 2018;35(4):723–30.
27. Zhang Q, Liu X, Gao M, Li X, Wang Y, Chang Y, et al. The study of human serum metabolome on the health effects of glyphosate and early warning of potential damage. Chemosphere. 2022;298:134308.
28. Barbosa ER, Leiros da Costa MD, Bacheschi LA, Scaff M, Leite CC. Parkinsonism after glycine-derivate exposure. Mov Disord. 2001;16(3):565–8.
29. Madani NA, Carpenter DO. Effects of glyphosate and glyphosate-based herbicides like Roundup™ on the mammalian nervous system: A review. Environ Res. 2022;214(Pt 4):113933.
30. Rueda-Ruzafa L, Cruz F, Roman P, Cardona D. Gut microbiota and neurological effects of glyphosate. Neurotoxicology. 2019;75:1–8.
31. Rebai O, Belkhir M, Boujelben A, Fattouch S, Amri M. Morus alba leaf extract mediates neuroprotection against glyphosate-induced toxicity and biochemical alterations in the brain. Environ Sci Pollut Res Int. 2017;24(10):9605–13.

32. Ait Bali Y, Madougou FA, Ba-M'hamed S, Giustetto M, Bennis M. Glyphosate-based herbicide exposure affects cognitive flexibility and social cognition in adult mice. Neurosci Lett. 2024;837:137912.
33. Ait-Bali Y, Ba-M'hamed S, Gambarotta G, Sassoè-Pognetto M, Giustetto M, Bennis M. Pre- and postnatal exposure to glyphosate-based herbicide causes behavioral and cognitive impairments in adult mice: evidence of cortical ad hippocampal dysfunction. Arch Toxicol. 2020;94(5):1703–23.
34. Cattani D, Cesconetto PA, Tavares MK, Parisotto EB, De Oliveira PA, Rieg CEH, et al. Developmental exposure to glyphosate-based herbicide and depressive-like behavior in adult offspring: Implication of glutamate excitotoxicity and oxidative stress. Toxicology. 2017;387:67–80.
35. Allegretto EA, Smeal T, Angel P, Spiegelman BM, Karin M. DNA-binding activity of Jun is increased through its interaction with Fos. J Cell Biochem. 1990;42(4):193–206.
36. Pan J, Zhao YX, Wang ZQ, Jin L, Sun ZK, Chen SD. Expression of FasL and its interaction with Fas are mediated by c-Jun N-terminal kinase (JNK) pathway in 6-OHDA-induced rat model of Parkinson disease. Neurosci Lett. 2007;428(2–3):82–7.
37. Ramírez-López F, García-Montes JR, Millán-Aldaco D, Palomero-Rivero M, Túnez-Fiñana I, Drucker-Colín R et al. Transcranial Magnetic Stimulation Attenuates Dyskinesias and FosB and c-Fos Expression in a Parkinson's Disease Model. Brain Sci. 2024;14(12).
38. Wang L, Yang YF, Chen L, He ZQ, Bi DY, Zhang L, et al. Compound Dihuang Granule Inhibits Nigrostriatal Pathway Apoptosis in Parkinson's Disease by Suppressing the JNK/AP-1 Pathway. Front Pharmacol. 2021;12:621359.
39. Cheng Q, Wang J, Li M, Fang J, Ding H, Meng J, et al. CircSV2b participates in oxidative stress regulation through miR-5107-5p-Foxk1-Akt1 axis in Parkinson's disease. Redox Biol. 2022;56:102430.
40. Liu K, An J, Zhang J, Zhao J, Sun P, He Z. Network pharmacology combined with experimental validation show that apigenin as the active ingredient of Campsis grandiflora flower against Parkinson's disease by inhibiting the PI3K/AKT/NF-κB pathway. PLoS ONE. 2024;19(10):e0311824.
41. Calogero AE, Soma PF, Giuffrida MC, Giuffrida D, La Vignera S, Romano C, et al. PARP1 and CASP3 gene expression in a patient with multiple head and neck squamous cell carcinoma and Parkinson disease. Hum Cell. 2013;26(1):44–6.
42. Sarawi WS, Attia HA, Alomar HA, Alhaidar R, Rihan E, Aldurgham N, et al. The protective role of sesame oil against Parkinson's-like disease induced by manganese in rats. Behav Brain Res. 2024;465:114969.
43. Yin S, Zhai Y, Song R, Wu J, Zhang Y, Yu M, et al. PARL stabilizes mitochondrial BCL-2 via Nur77-mediated scaffolding as a therapeutic strategy for Parkinson's disease. Cell Death Dis. 2025;16(1):700.
44. Zhang Y, Wu Q, Zhang L, Wang Q, Yang Z, Liu J, et al. Caffeic acid reduces A53T α-synuclein by activating JNK/Bcl-2-mediated autophagy in vitro and improves behaviour and protects dopaminergic neurons in a mouse model of Parkinson's disease. Pharmacol Res. 2019;150:104538.

45. Ma Q, Tian JL, Lou Y, Guo R, Ma XR, Wu JB, et al. Oligodendrocytes drive neuroinflammation and neurodegeneration in Parkinson's disease via the prosaposin-GPR37-IL-6 axis. Cell Rep. 2025;44(2):115266.
46. Borsche M, König IR, Delcambre S, Petrucci S, Balck A, Brüggemann N, et al. Mitochondrial damage-associated inflammation highlights biomarkers in PRKN/PINK1 parkinsonism. Brain. 2020;143(10):3041–51.
47. Sun MF, Zhu YL, Zhou ZL, Jia XB, Xu YD, Yang Q, et al. Neuroprotective effects of fecal microbiota transplantation on MPTP-induced Parkinson's disease mice: Gut microbiota, glial reaction and TLR4/TNF-α signaling pathway. Brain Behav Immun. 2018;70:48–60.
48. Kim TW, Koo SY, Riessland M, Chaudhry F, Kolisnyk B, Cho HS, et al. TNF-NF-κB-p53 axis restricts in vivo survival of hPSC-derived dopamine neurons. Cell. 2024;187(14):3671–e8923.
49. Sutherland G, Mellick G, Newman J, Double KL, Stevens J, Lee L, et al. Haplotype analysis of the IGF2-INS-TH gene cluster in Parkinson's disease. Am J Med Genet B Neuropsychiatr Genet. 2008;147b(4):495–9.
50. Qin X, Zhang X, Li P, Wang M, Yan L, Pan P, et al. MicroRNA-185 activates PI3K/AKT signalling pathway to alleviate dopaminergic neuron damage via targeting IGF1 in Parkinson's disease. J Drug Target. 2021;29(8):875–83.
51. Yang L, Wang H, Liu L, Xie A. The Role of Insulin/IGF-1/PI3K/Akt/GSK3β Signaling in Parkinson's Disease Dementia. Front Neurosci. 2018;12:73.

Figures

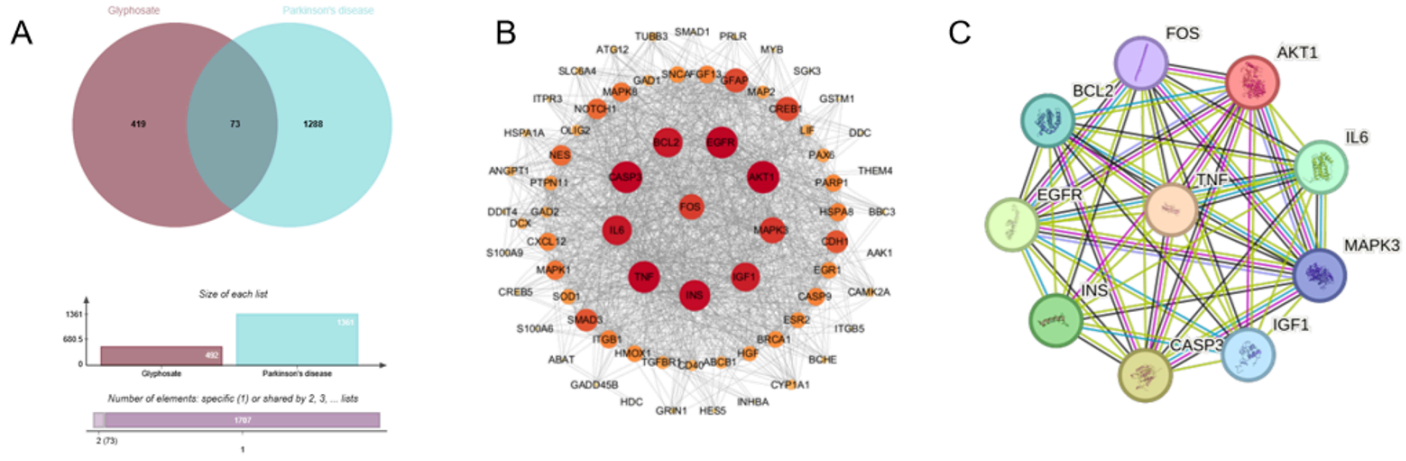


Figure 1

Network toxicology analysis. (**A**) Venn diagram visualizing the common targets shared by the compound and the disease. (**B**) PPI network of the common targets. (**C**) PPI network of the ten targets.

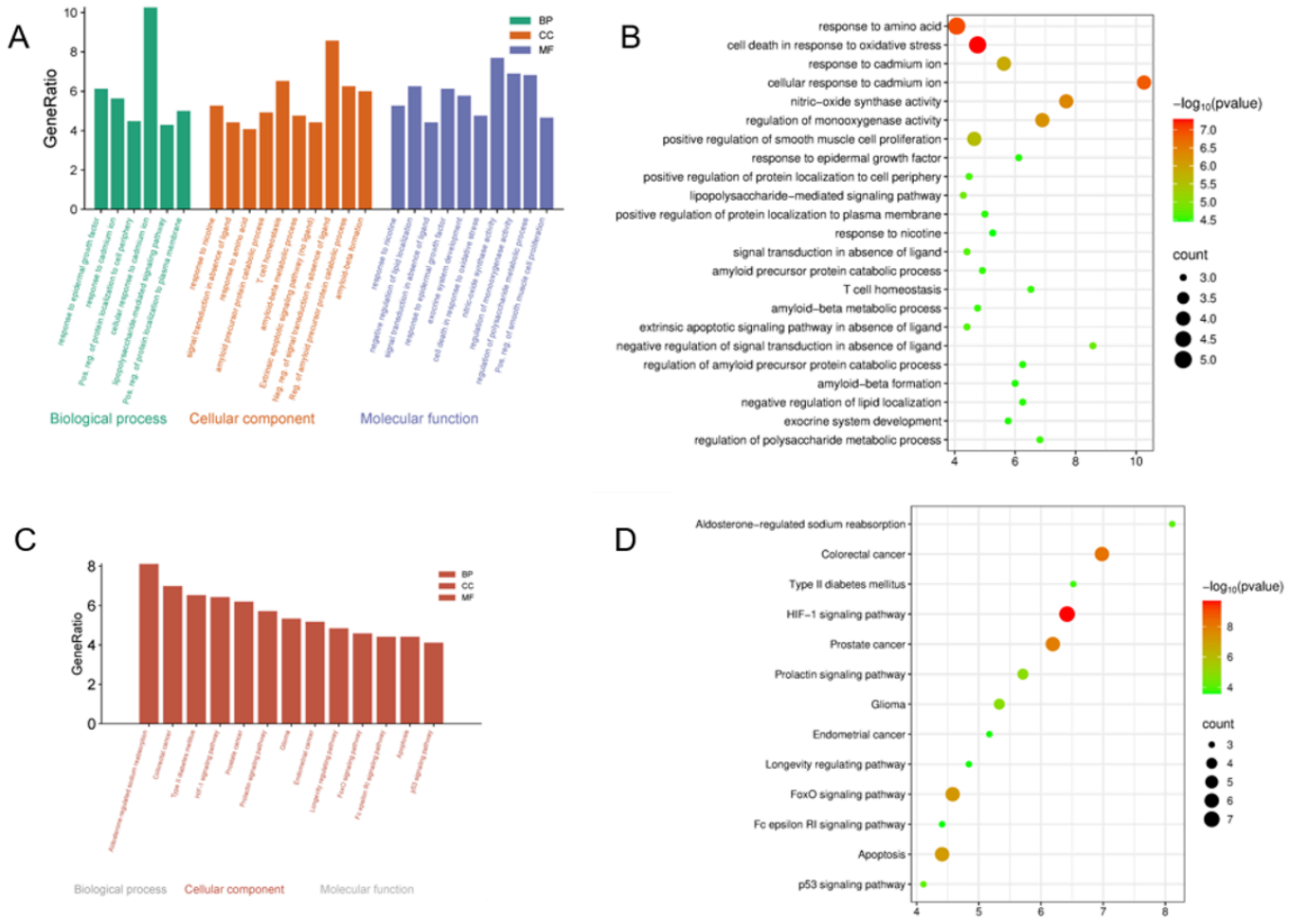


Figure 2

GO functional enrichment and KEGG pathway analysis. (**A**) Bar chart of GO analysis, the x-axis represents the number of overlapping targets enriched in each term, and the y-axis denotes the names of GO terms. Green indicates biological process (BP), orange represents cellular component (CC), and blue stands for molecular function (MF). (**B**) Highly enriched GO terms. (**C**) Bar chart of KEGG pathway analysis. **(D)** Highly enriched KEGG terms were selected from the target list based on their enrichment levels. The size of the circles corresponds to the number of enriched protein targets, while the color of the circles indicates the statistical significance of the differences.

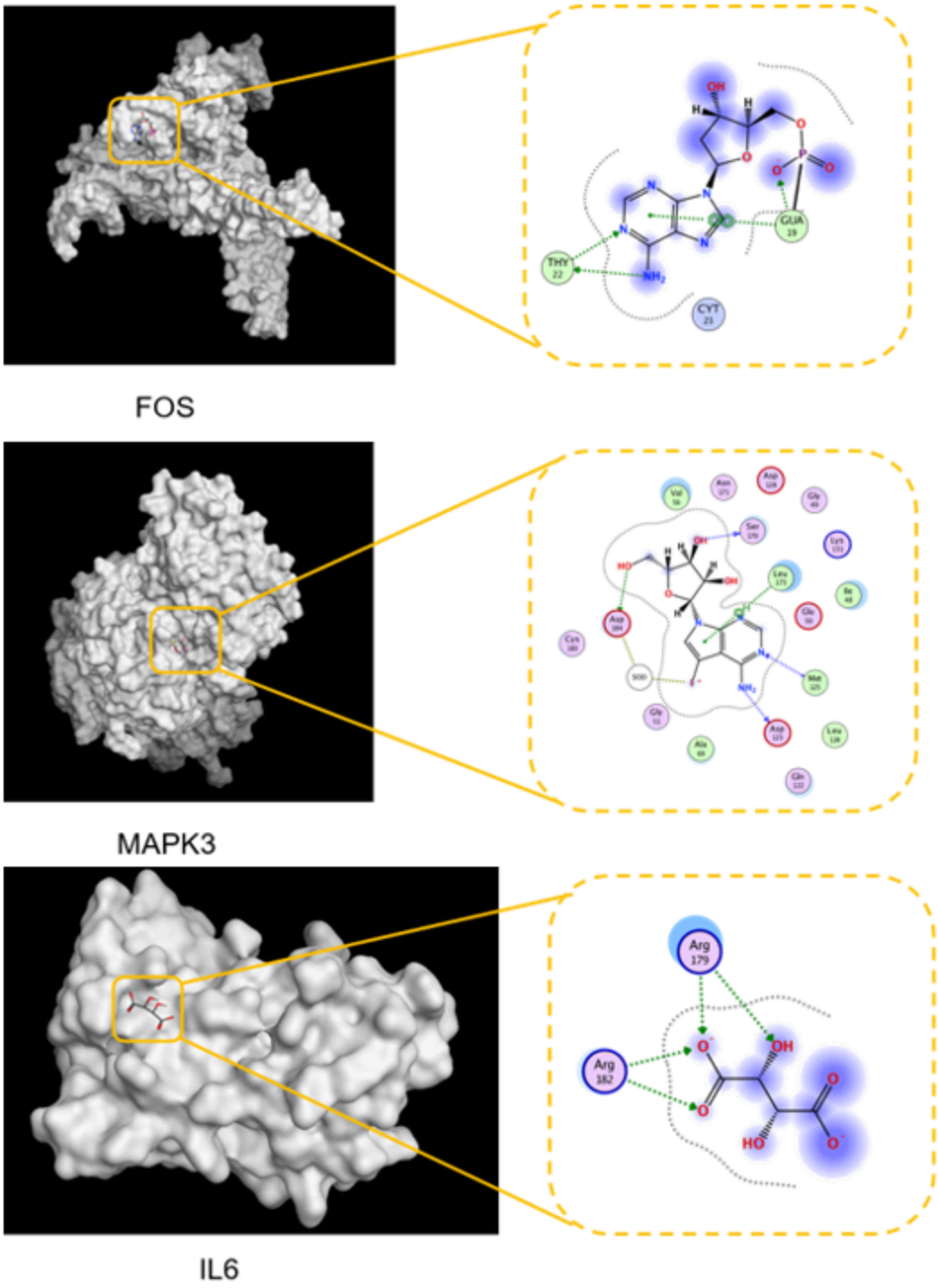


Figure 3

Molecular docking models. (A) Glyphosatewith FOS; (B) Glyphosate with MAPK3; (C) Glyphosatewith IL6.

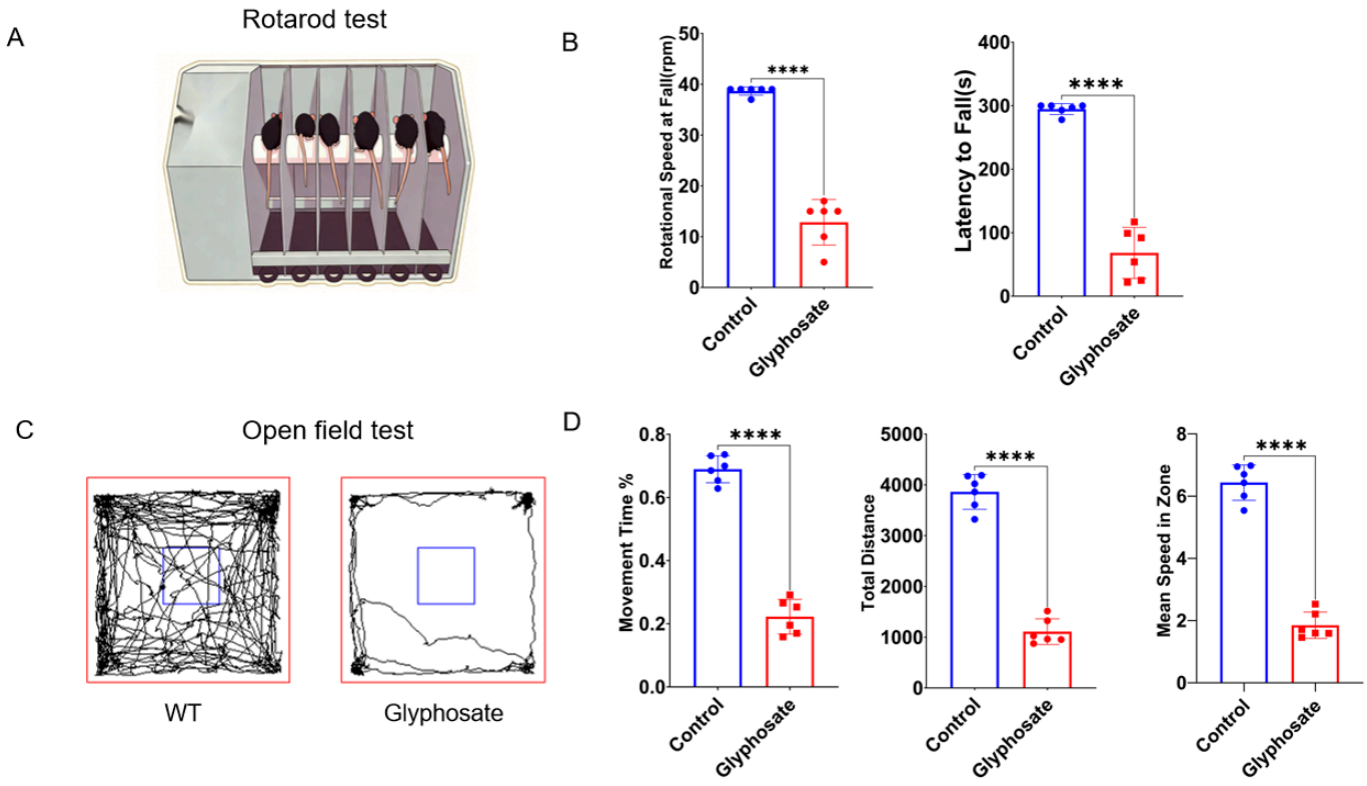


Figure 4

Behavioral test results of mice in the control group and glyphosate-induced model group

(A) Rotarod test schematic diagram. (B) Rotarod test for assessing motor coordination and balance in mice. (C) Representative diagrams of mouse movement trajectories in the open field test. (D) Open field test for evaluating spontaneous activity in mice. All results are presented as the mean ± SEM(n=6). ∗∗∗∗*P*<0.0001

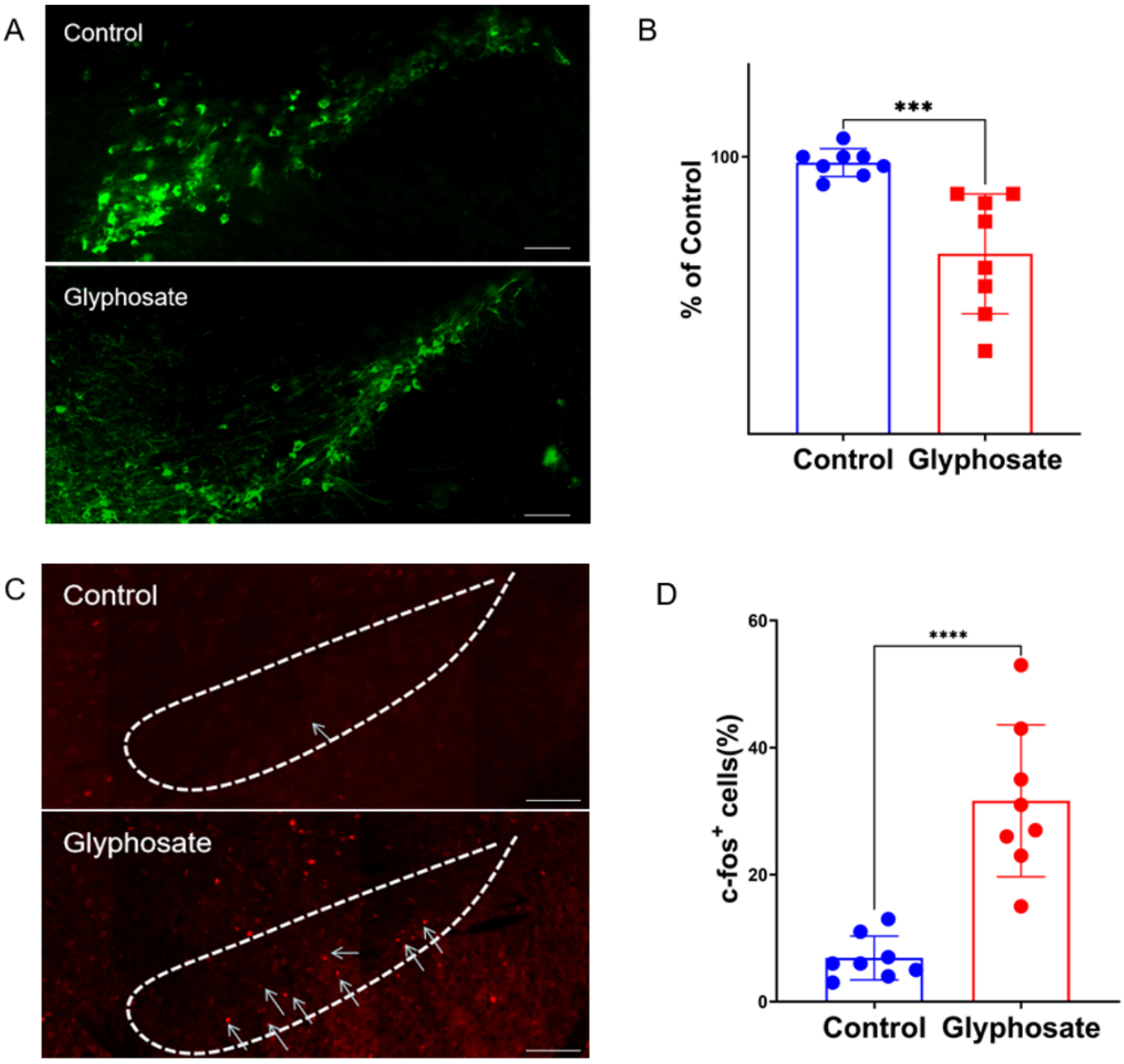


Figure 5

(A) Representative images showing tyrosine hydroxylase (TH)-positive neurons in the substantia nigra pars compacta of control and glyphosate-treated mice. (B) Stereological quantification of TH-positive dopaminergic neurons in the SNc. (C) Representative images showing c-Fos immunoreactivity in the SNc of control and glyphosate-treated mice; white arrows indicate c-Fos-positive nuclei. (D) Quantification of the percentage of c-Fos-positive cells in the SNc. Data are presented as mean ± SEM (n = 8 per group). ***p < 0.001, ****p < 0.0001 vs. control group, unpaired t-test. Scale bar = 100 μm.